

# A simple review of quantum communication and quantum communication experiments in three different mediums

Siyuan Ji

RDFZ Chaoyang Branch School, Beijing, China

**Abstract:** Quantum communication is an implementation based on quantum mechanics. This includes quantum entanglement theory, quantum cryptography, quantum teleportation, quantum repeater, and quantum storage. All components of quantum communication except entanglement are reviewed in this paper. Besides, this paper discusses three different media, land, underwater and space, in which quantum communication can be operated. Quantum communication on land and underwater uses optical fibers, and quantum communication in space uses satellites. In this paper, two experiments for each of these three media are carried out to illustrate how quantum communication is established on these three media. Thus, quantum communication and its three media are reviewed in this paper.

**Keywords:** Quantum communication, quantum teleportation, information transmission

## 1. Introduction

Quantum communication is an implementation based on quantum mechanics, includes theory of quantum entanglement, quantum cryptography, quantum teleportation, quantum repeater, and quantum memory. In this paper, except quantum entanglement, all the components involved in quantum communication are reviewed. In addition, this paper is discussing three different mediums where quantum communication can be set up, which are, land, underwater, and space. Land-based and underwater-based quantum communication are using optical fibers, and quantum communication in space is using satellites. The paper uses two research experiments for each medium to explain how quantum communication is set up within these three mediums. Consequently, this paper achieved to review the quantum communication and its three mediums of it.

## 2. Cryptography

The first protocol for quantum communication was proposed in 1984 by Charles H. Bennett, named BB84.[3] The protocol consists of four quantum states containing two different bases: the state  $|up\rangle$ ,  $|down\rangle$ ,  $|right\rangle$ ,  $|left\rangle$ . Conventionally, people define the state  $|up\rangle$  and  $|right\rangle$  with a value 1, and  $|down\rangle$  and  $|left\rangle$  with the value 0 as shown in Figure 1.

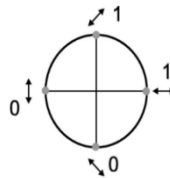


Figure 1: Implementation of the Bennet and Brassard (BB84) protocol. The four states lie on the equator of the Poincaré sphere.

At first, sends a photon with polarization in random of the four states in Figure1. to Bob, the receiver. (In Fig 1, the state  $|up\rangle$ , means polarization with  $+45^\circ$ , thus the four states are “Horizontal”, “Vertical”, “ $+45^\circ$ ”, “ $-45^\circ$ ”). Then, when Bob receives the photon, he measures the photon with one of the two bases. Whenever Alice the sender and Bob the receiver used the same base for measuring the photon, they get perfectly correlated results, and when using a different basis for measuring, they obtain an uncorrelated result. Alice and Bob know which bits are correlated in this protocol, as they used the same basis for measuring. Hence, a strategy is established following this: Bob announced the basis he used to measure

the photon in public. Alice then reveals whether or not the basis that the qubit she used for encoding is compatible with Bob's announcement. They keep the bit if it is compatible and abandoned it if not. By doing this in this method, about 50% of bit strings are discarded. The channel that Alice and Bob are using for communication is public, which is not secured. Then there is an opportunity for the eavesdroppers Eva to know the basis they are using, but if Bob didn't receive an expected qubit, he will communicate with Alice to disregard it. Thus, Eva didn't get useful information, but only lowered the bit rate. The term *bit rate* is basically the number of bits which can be transmitted in a second. [9]. Ideally, Eva would send a copy of the photon with its original state to Bob while keeping a copy of the photon for herself.

### 3. Quantum teleportation

To understand quantum communication, we have known how information are encrypted now, how to transmit the information is a problem. As communication requires the ability to send information from one place to another, quantum teleportation was introduced for quantum communication. The whole process constitutes three steps. First, there is a pair of entangled photons with the  $|\text{EPR}\rangle$  state (or called Bell's state) sent through optical fibers as shown in Figure 2. A "quantum teleportation channel" is established. Second, the sender operates an action called Bell state measurement (BSM). BSM is a complete set of orthogonal entangled state projected by a state of two two-level systems [13] between his photon from the entangled resource with the qubit that contains information needed to be teleported, which have been testified [4]. However, the Bell state measurement only tells the relationship between the two photons, but communication requires the exchange in information. [1] Thus, third, Alice informs Bob of her Bell state measurement result, and Bob operates his photon by changing the phase or changing the amplitude, which bob will know Alice's photon. After this operation, the teleportation is finished.

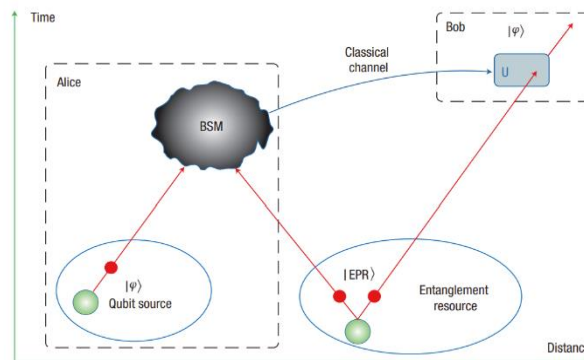


Figure 2: Illustration of quantum teleportation

### 4. Quantum repeater

The process that teleporting the entangled state is known as quantum swapping [20]. The general idea is that by creating entanglement at two close nodes, then teleporting the entanglement from one to the other, which is known as a quantum relay [12], the detailed process is shown in Figure 3. However, the distances can be achieved by quantum relays are limited, owing to we need to create 2 pairs of entangled photon to connect a pair of photon as explained above, and quantum relays are not helping with increasing bit rate. [8]. At this time, because people are unable to overcome the distance limitation, the idea of a quantum repeater is introduced by H.-J. Briegel, W.D ür, J.I Cirac and P. Zoller in 1998. [5] The general idea is that, as shown in Figure 4, by using a suitable apparatus to store entanglement state and send to the other station point, thus the distance will not be limited because we can used infinite numbers of apparatus to store the entanglement state and send to the other [6].

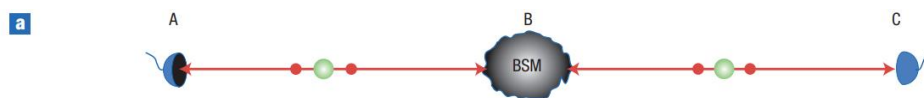


Figure 3: The process of quantum relay

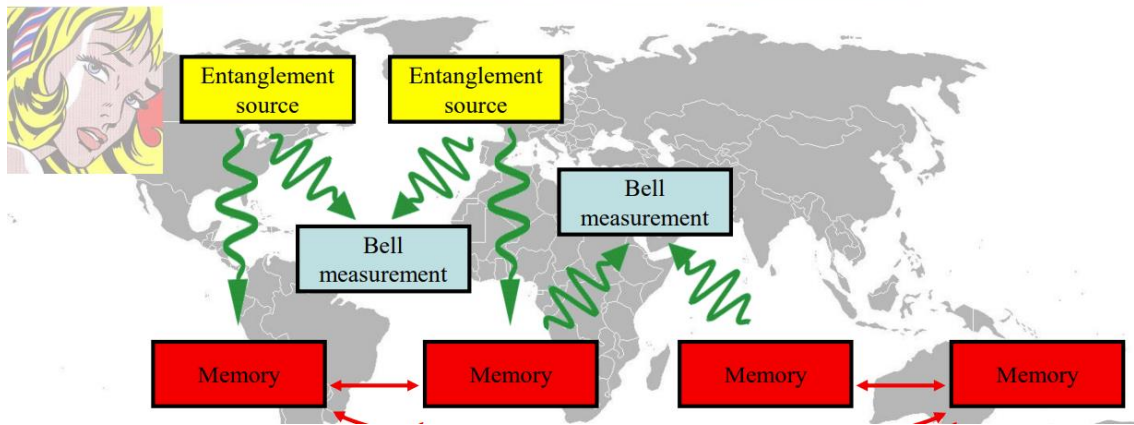


Figure 4: Quantum repeater's process

### 5. Quantum memory

Quantum memory's main use is for the quantum repeater, while there are other uses, that are outside the scope of this paper<sup>[7]</sup>. The basic idea is that by using electromagnetic-induced transparency (EIT) medium, shown in Figure 5. Electromagnetically induced transparency is a quantum interference effect that permits the propagation of light through an otherwise opaque atomic medium<sup>[15]</sup> turning off the control field can make the group velocity zero, as shown in Figure 6. This means that the velocity of the photon in the EIT medium are reducing to zero, and accomplished to store the photon inside the EIT medium. Then the quantum information stored in the photon is stored in the EIT medium. Turning the control field back will retrieve the pulse in the original state<sup>[16]</sup>. The total process is demonstrated virtually in Figure 7.

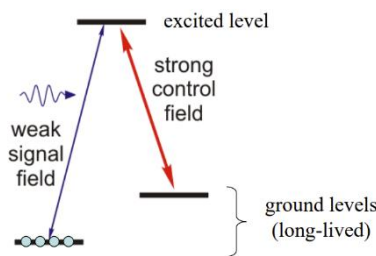


Figure 5: The model of quantum memory

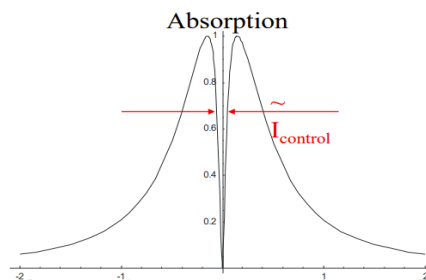


Figure 6: Absorption of the signal field

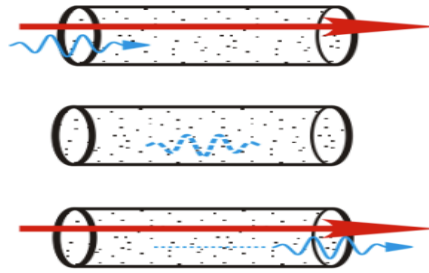


Figure 7: EIT for quantum memory

## 6. Medium: Optical fibers on land

Sebastian Phillip Neumann and his team published research about quantum communication over a 248km fiber link.<sup>[18]</sup> Namely, a distance of 248km quantum communication by using telecom fiber to connect Bratislava(B) in Slovakia and St. Pölten(SP) via Vienna in Austria. Despite a total loss of 79 dB, they achieved entangled pair rates of  $9 \text{ s}^{-1}$  and secure key rates of 1.4 bits/s on average, with stabilized state of 110 hours. In a word, they achieved a stable, high-fidelity, and high efficiency quantum communication over a long distance.

The entangled photon pairs are formed by first, deploying a Sagnac-type source based on spontaneous parametric down-conversion, which is a photon spontaneously splitting into two photons of lower energy a nonlinear optical process inside a ppLN crystal. A Sagnac-type source is a photon with the phenomenon caused by rotation encountered in interferometry found by Georges Sagnac. Next, use two 100 GHz wavelength division multiplexing channels. The source was operated at 422 mW pump power, with less than 0.4% erroneous polarization measurements in a laboratory environment.

The apparatus at SP and B are identical in construction and each contains a bulk polarization measurement module (PMM), a 4-channel superconducting nanowire single-photon detector (SNSPD), and time-lagging electronics (TTM). Although the environment in the laboratory does not constitute a long-distance link, the losses in source PMM and SNSPD are set up. In this way, the accuracy of the experiment is ensured, by using those high-accuracy apparatus and simulate the losses in practical.

In the PMM, coupled photons collide with a 50:50 beamsplitter randomly directing them to two impartial linear polarization basis measurements. By setting the 50:50 beamsplitter, they are able to provide a situation where the probability of a split photon is 50%. The first basis is realized by a PBS transmitting (reflecting) the horizontal (vertical) polarization mode. The second basis is the diagonal basis. All events that are detected are measured by TTM with 1 ps resolution. There are two TTM at both SP and B, and each TTM is disciplined to a GPS clock, as a result, the relative delay of this clock is on average, 13 ps/s. Providing the experiment setting would show how they set the apparatus in order to guarantee accuracy. However, the polarization measurement error along the link (2.6 %) is higher than in laboratory measurements (0.2 %) mainly due to keeping the PPC alignment time low. Measurements with an optical time-domain reflectometer (OTDR) of the fiber to St. Pölten (Bratislava) yielded a fiber length  $L$  of 129.0 km (119.2 km) and losses of  $-31.9 \text{ dB}$  ( $-32.6 \text{ dB}$ ). In addition to the loss, the long-distance optical fiber of QKD also includes the influence of dispersion (CD) and polarization mode dispersion (PMD). In conclusion, they cannot observe the polarization fidelity loss caused by polarization mode dispersion in the fiber link.

On the other hand, H Takesue and his team published an experiment that, examined the different phase shifts of QKD over 105 km fiber.<sup>[11]</sup> They used a pulse train with a 1GHz frequency with a phase difference of  $\pi$ , and the receiver obtained the signal after attenuation. The entire process is shown in Figure 8. The insertion loss in the interferometer was 2.5dB, and each click at the photon counters was recorded by using a time interval analyzer.

To maximize the secure key generation rate, they set the average photon number to the optimum value for each transmittance with their expected value. The pump power was set up for bit errors caused by dark count. To reduce the impact of false clicks due to the amplification of the received signal, they applied a time gating to the recorded data, which also reduces the effective dark count per time gate. Figure 9 shows the secure key generation rate as a function of fiber length, where the square represents

the secure key generation of fiber transmission. X means the experimental result simulating a fiber loss with an optical attenuator with the time window at 8.8% and 0.6ns, which reduced the detection efficiency by 33%. The total dark count rate was 26kHz.

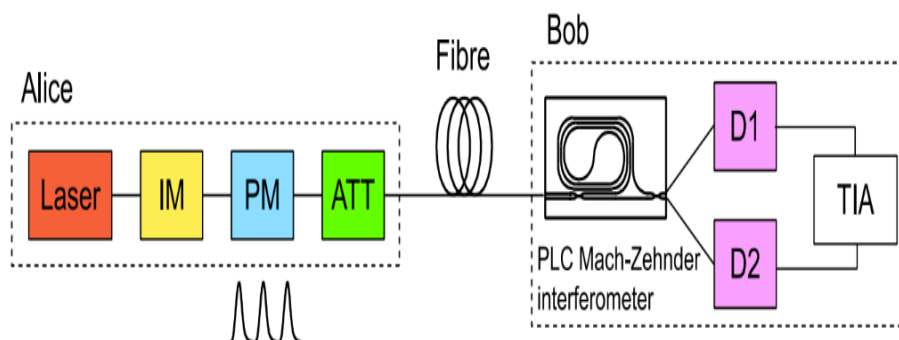


Figure 8: The process of H Takesue's experiment

At 30km or less fiber lengths, they achieved a sifted key generation rate of more than 1Mbit/s, which is twice more than the research published by Yoshizawa A, Kaji R, and Tsuchida H in 2004. [19] Then they redo the experiment with 3mW pump powers, 2% quantum efficiency, 2.7kHz dark count, and a time window of 0.2 ns. While using the time window of 0.2 ns, the detection efficiency was reduced by 55%. By using the setup value mentioned above, their result is, a 209 bit/s secure key rate, and the bit error rate was 7.95% at 105km. In conclusion, the experiment is high-efficiency, with a relatively low error rate.

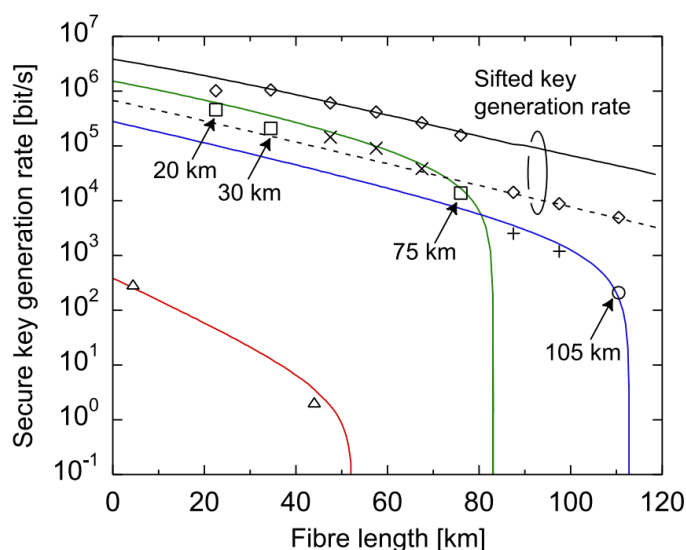


Figure 9: Experiment result

## 7. Water

Shanchuan Dong and his team established an underwater condition for quantum key distribution based on the decoy-state BB84 protocol. [3]

The team used a 450nm laser to identify energy loss. The channel is a 2.4m toughened glass tank filled with water with controlled water quality, which avoided error in result caused by different water quality or impurities. The average temperatures were maintained at 15°C. However, they haven't considered attenuation caused by water turbulence.

The decoy-state QKD needs three different intensities of lights. Dong and his team set the average photon number per pulse of the signal state to 0.8 and the decoy-state to 0.1, with zero photon number in the vacuum state. The relationship between 4-bits random number and photon state are shown in Table 1.

Table 1: Relationship of 4 bits and its photon state

Bit <sub>0</sub>	Bit <sub>1</sub>	QuantumState	Bit <sub>2</sub>	Bit <sub>3</sub>	PolarizationState
0	0	VacuumState	0	0	H
0	1	DecoyState	0	1	V
1	0	SignalState	1	0	P
1	1	SignalState	1	1	M

After calibrating the quantum laser module, they send all the polarized states that have been prepared to testify the fidelity of these states. The average value of polarization state fidelity is 98.574%, which demonstrates that their method is capable of proceeding with subsequent QKD procedures. Then they redo the experiment with 3 different attenuations with 10.22dB, 12.36dB, and 14.4dB. The parameters and the average final key rate are shown in Table 2. The system is experimented with attenuation of 16.35 and changes the number of photons per pulse to 0.7 for verifying the design that Dong and his team can calibrate the trigger intensity of the signal state and decoy-state independently. Thus, their experiment can be tested for various parameters.

Table 2: Experiments parameters and result (Dong et al, 2022)

Attenuation	Q <sub>u</sub>	E <sub>u</sub>	Q <sub>v</sub>	Q <sub>1</sub>	E <sub>1</sub>	Finalkeyrate(bits/s)
10.22 dB	1.48×10 <sup>-2</sup>	1.21%	1.89×10 <sup>-3</sup>	4.84×10 <sup>-3</sup>	1.18%	3535.7
12.36 dB	6.97×10 <sup>-3</sup>	1.64%	8.76×10 <sup>-4</sup>	1.94×10 <sup>-3</sup>	0.71%	826.4
14.40 dB	3.70×10 <sup>-3</sup>	1.62%	4.90×10 <sup>-4</sup>	1.01×10 <sup>-3</sup>	1.52%	404.6
16.35 dB	1.47×10 <sup>-3</sup>	2.20%	2.17×10 <sup>-4</sup>	5.51×10 <sup>-4</sup>	1.91%	245.6

Next, by calculation of the equation from “Practical decoy state for quantum key distribution” [17], Dong and his team made a graph about the relationship between secure key rate and water channel distance as shown in Figure 10. From the graph, for different parameters, the secure key rate decreases at different rate. The maximum distances can be achieved by their experiment is around 330 to 340 meters.

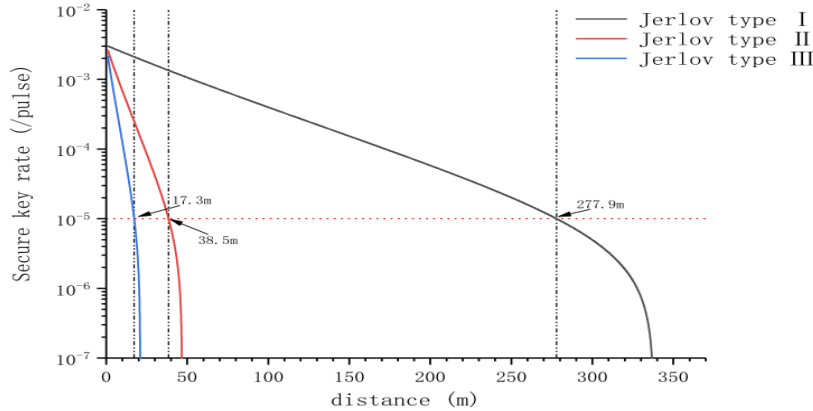


Figure 10: The relationship between secure key rate and underwater channel distance

Felix Hufnagel and his team published research that involve quantum communication with the underwater medium as well.<sup>[10]</sup> In their research, still, the sender and receiver, but in the channel that is underwater with a flume tank which has a depth of 50 meters. There was a trolley on the top of the flume, which can travel in the channel with Alice’s setup. The sender consists of transmitting polarization state and transmitting spatial structure mode.

A polarizing beamsplitter was sent with a 532nm diode. A mean photon number of 0.1 photon/ns was achieved by the neutral density filters attenuating the beam. A 3-inch lens was used for collecting the beam initially. The whole beam is focused, even with a slight beam drift, because of underwater turbulence. The beam then passes through a wave plate with  $\lambda/2$  and  $\lambda/4$ , then through the polarization beamsplitter to project the entangled state to a specific state. Next, the beams are then coupled to a single-mode fiber connected to a single-photon avalanche diode detector. The setup was initially optimized to place the trolley 1 meter away from the receiver.

From the experiment, the relation between distance, quantum bit error rate (QBER), and the key rate

is shown in Table3, which shows that there is a slight increase in QBER with an increase in distance, though the QBER at 20.5 meters is not precise with other data. The main reason for the increase in error is the loss caused by long-distance turbulence. Then the experiment was repeated with a vector vortex beam, the relationship is shown in Table 4.

Table 3: Quantum bit error rate and key rates for polarization BB84

Distance	0.5m	10.5m	20.5m	30.5m
QBER(%)	0.27	0.74	3.7	0.96
Key rate	0.94	0.87	0.54	0.84

Table 4: Quantum bit error rate and key rates for a two-dimensional BB84 using vector vortex beam

Distance	1.5m	5.5m	10.5m
QBER(%)	1.44	3.4	1.0
Key rate	0.79	0.57	0.84

They also studied the effect of underwater turbulence on the space distribution of vector vorticity modes spreading through different channel lengths. A CCD camera was used for measuring the intensity of the beam, performing polarization tomography. The phase distortion associated with turbulence includes not only an oblique aberration but also astigmatism and other high-order effects on the spatial profile of the beam. Underwater aberrations are slower than observed. Astigmatism is thus easier to see in a free air space than the scintillation that is often observed under strong turbulence in the air.

In the data analysis section, the research plotted a graph as shown in Figure11, the relationship between secret key rate and channel length. The black curve shows the optimal key rate for measuring the attenuation of the underwater channel. The red points are the experiment result. Although the experimental point is lower than the zero QBER theory, it is approximate with the theoretical line and supports the prediction of 80 meters. The dashed line shows the expected optimal key rate when the channel length exceeds 30 meters. The maximum calculation is accomplished by using the parameters in Table5.

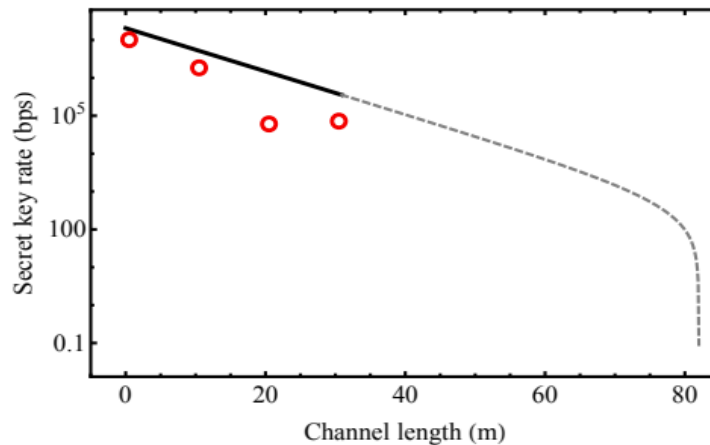


Figure 11: Secret key rate for the underwater polarization channel

Table 5: Experimental parameters of the underwater polarization channel

Parameter	Dark Counts	Source Rep Rate	Detector Efficiency	Bob's Detection Efficiency	Channel Loss( $\alpha$ )
Flume Result	300 Hz	$10^9$ Hz	0.6	0.188	0.57dB/m

The optimal key rate is shown as black, taking into account only errors caused by the dark count. When the channel length is 0.5, 10.5, 20.5, and 30.5 m, the measured QBER is added to the experimental data points of background error and shown in red. The key rate analysis of the vector vorticity mode is as follows. The exact method of the polarization state is proved. The only change is the experimentally observed QBER, which is similar to the value of a polarization channel of the same length -- around 1% for a 10 m channel -- thus yielding similar key rates. For example, the vector vortex mode has a critical rate of 72kbps for a 10.5 m channel. In conclusion, they have performed an underwater channel which maintained its fidelity in both the polarization and vector vortex state. In addition, they have proven that

their channel is able to use in an underwater free-space setting.

## 8. Satellite

Quantum communications in space are usually set up with using the satellite. Mainly, by teleporting the entangled photon from ground to satellite, or from satellite to satellite.

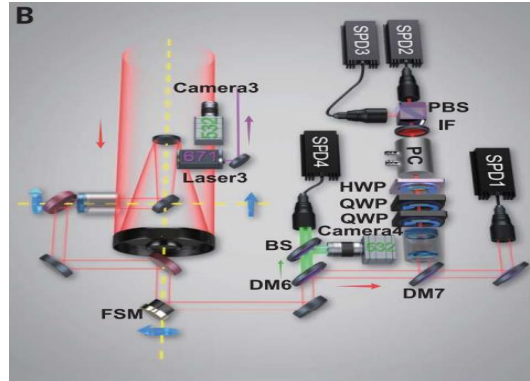


Figure 12: A near-diffraction-limited far-field divergence of  $\sim 10$  mrad by two Cassegrain telescopes with apertures of 300 and 180 mm

Liao and his team published a paper about satellite-based entanglement that has propagated over 1200 km.<sup>[14]</sup> An efficient method is required because the entangled photon cannot be amplified, and due to the channel loss caused by factors like air turbulence or beam diffraction. By combing a beam divergence with high-bandwidth and high-precision acquisition pointing tracking (APT) technique, they built up a closed-loop APT system in both the transmitter and receivers, as shown in Fig 9 and Fig 10. The entire optical efficiency between the two telescopes is 45% to 55%, the experiment has achieved quantum entanglement distribution both between Delingha and Lijiang and between Delingha and Nanshan. When starting the APT system, the satellite reached an elevation of 5 degrees and, at the beginning of the measurement, it reached an elevation of  $10^\circ$ .

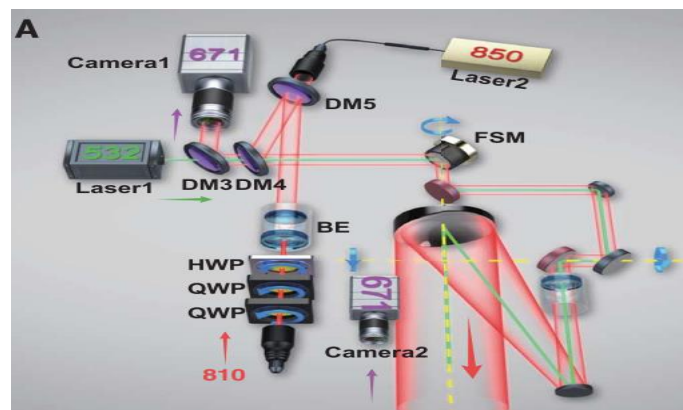


Figure 13: The receiver (Liao et al, 2017)

Owing to the motion of the satellite, a drift in the time difference and polarization rotation was caused. However, by using a combination of motorized wave plates for dynamic polarization compensation, a polarization contrast of 80:1 was obtained. In addition, a 100-kHz pulsed laser was used for the synchronization of the two ground stations. Beyond that, they placed 20-nm bandwidth filters to control the background noise, and in the experiment, the background noise is 500 to 2000 counts/s due to the position of the Moon.

The satellite flies along a sun-synchronous orbit and meets Delingha and Lijiang's view once every night. The distance between the satellite and Delingha and Lijiang is shown in Figure11, which demonstrates the overall channel length of the two stations. They measured the downlink attenuation ranging from 64 to 82dB and observed an average two-photon count rate of 1.1Hz.

Except Liao's experiment, there was an experiment that considered different satellite channel in 2003. The experiment tested the QKD through satellite by satellite to ground and satellite to satellite links.<sup>[2]</sup>



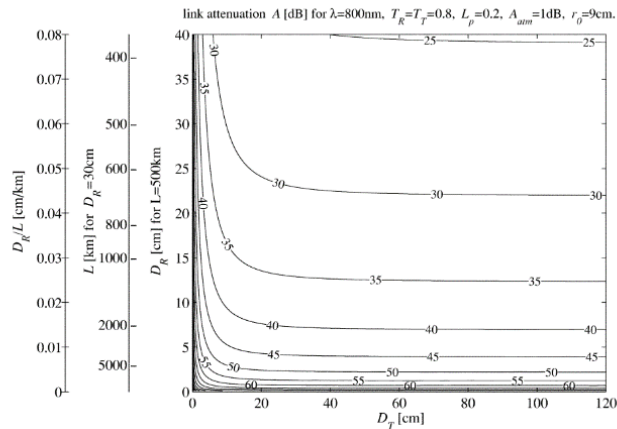


Figure 14: A contour plot of link attenuation as a function of transmitter and receiver

First of all, the satellite to ground links. In the low earth orbit case, they claimed that link-attenuation is not a problem. Figure 14 plotted a rough diagram between the link attenuation and the receiver aperture diameter for  $\lambda=800$  nm. A link distance  $L$  for 30 cm receiver telescope aperture and receiver telescope aperture for link distance  $L=500$ km were given for the additional vertical scale. In the case of the link connecting the LEO and the ground station, the possible communication duration is relatively short, and the angular velocity at which the telescope at the ground station must move to track the satellite along its orbit is high. However, the long-distance link between geostationary orbits has high attenuation. As a result, the diameter is 100cm at the ground station aperture and the diameter is 30cm at the geostationary orbit terminal aperture, only one will meet the attenuation requirement of 60dB.

## 9. Discussion

In Neumann's experiment, he used a ppLN crystal to create a pair of the entangled photons and used time-lagging electronics to record the observation, for reducing the error in observation. While in laboratory condition, they have maintained the secure key rates of 1.4 bits/s on average, with stabilized state of 110 hours with an entangled pair rate of 9/s. Those are the advantages of their research.

However, the polarization measurement error along the link is higher than in laboratory measurements mainly due to keeping the PPC alignment time low, and they were unable to observe the loss of polarization fidelity due to polarization mode dispersion in the fiber link.

In H Takesue's experiment, they set the average number of photons to the optimal value of each transmittance and its expected value to maximize the secure key generation rate, which differs from Neumann's experiment. In addition, they applied time gating to record the data to reduce the dark count, which used the same method as Neuman's except for the equipment.

For quantum communication underwater, Shanchuan Dong and his team used a 450nm laser to identify energy loss. The channel is a 2.4m tempered glass tank filled with water of controlled quality. The average temperature remains at 15 °C.

On the other hand, the turbulence was not observed yet, as they have mentioned in their paper. Moreover, they are facing some practical issues. The most important of these is the alignment between sender and receiver, which they said they are working on but not implementing in their research.

In Felix Hufnagel's experiment, an advantage is that they have considered water turbulence. They have investigated the effect of underwater turbulence on the spatial distribution of vector vorticity modes propagating through different channel lengths, which can make them demonstrate how water turbulence affects the distribution. However, having a gathered-up diagram to represent the relationship between distance, water turbulence, and QBER.

Juan Yin's experiment about satellite-based quantum communication builds closed-loop APT systems in both the transmitter and receivers to maximize the link efficiency, which is affected by channel loss due to air turbulence or beam diffraction. To control the background noise, they placed a 20 nm bandwidth filter. Compared to previous entanglement distribution methods using the best performing (0.16 dB/km loss) and most common (0.2 dB/km loss) commercial telecom fiber direct transmissions,

respectively, from the same two-photon source - our satellite-based method using 12 at 275 seconds 17 orders of magnitude improvement in effective link efficiency within the coverage time.

The experiment established by Markus Aspelmeyer, Thomas Jennewein, and Martin Pfennigbauer, has considered a different condition of satellite-based quantum communication. The low earth orbit method doesn't require attenuation as they have explained, and the geostationary orbits have high attenuation, so they have used a smaller diameter for the fiber to meet the 60 dB attenuation requirement.

Beyond the experiments, this paper has reviewed the prerequisite theory of quantum communication. Explaining quantum cryptography, and demonstrated the BB84 protocol established by Charles H. Bennett in 1984, which is a frequent used protocol in quantum communication.

In addition, common idea of setting up the quantum teleportation, which used Bell state measurement to make a source bit entangled with the prepared entangled photon, and sent to the receiver the Bell state measurement result. The receiver then change the phase difference and amplitude of the photon. In this way, they achieved a way that the sender don't need to observe his photon's state but able to transform his information toward the receiver.

Last, this paper illustrated a method for extending distance limitation of quantum teleportation, which is quantum repeater, and the technique of quantum repeater, which is quantum memory. Quantum memory is basically, controlling the speed of photon travelling in the EIT medium to zero, which made the photon stored in the medium. With the help of quantum memory, quantum teleportation used this to store the entangled state, and send to other station point to extend the distance of quantum teleportation.

## 10. Conclusion

In conclusion, this paper has shown the basis theory for quantum communication and explained the principles of quantum cryptography, and quantum teleportation. Moreover, we discussed three different mediums of the quantum communication channel, which is orthogonal fiber channel on land, fiber channel underwater, and satellite-based quantum communication, and evaluated their experimental data with their advantages and shortages, and a few suggestions for the shortages.

For each of the mediums we have mentioned two research articles, for quantum communication on land, I used the experiment established by Sebastian Phillip Neumann, a experiment published in March 2022, which means that this experiment is a sort of most up to date distance that scholars are able to achieve. While H Takesue's experiment used massive skills to avoid errors in their experiment, for example the dark counts.

Next, for underwater conditions, Shanchuan Dong's experiment represent the newest finding of the underwater quantum communication, and used a set of technique to make the underwater communication precise like the time gating. Felix Hufnagel and his team is advantaged at, a depth of 50m tank, which is much greater that Dong's condition, and researched on how the water turbulence affect the loss of key rate. Moreover, their experiment was experimented in both the polarization and vector vortex state.

Finally, for satellite-based quantum communication, Juan Yin and his team and the research done by Markus Aspelmeyer, Thomas Jennewein, and Martin Pfennigbauer were used to show their different method.

## References

- [1] Acín, A., Gisin, N., & Masanes, L. (2006, September 20). From Bell's theorem to secure quantum key distribution. *Physical Review Letters*. Retrieved April 27, 2022, from <https://journals.aps.org/prl/abstract/10.1103/PhysRevLett.97.120405>
- [2] Aspelmeyer, M., Jennewein, T., Pfennigbauer, M., Leeb, W., & Zeilinger, A. (2003, May 19). Long-distance quantum communication with entangled photons using satellites. *arXiv.org*. Retrieved May 6, 2022, from <https://arxiv.org/abs/quant-ph/0305105>
- [3] Bennett, C. H., & Brassard, G. (2020, March 14). *Quantum cryptography: Public key distribution and coin tossing*. *arXiv.org*. Retrieved April 27, 2022, from <https://arxiv.org/abs/2003.06557>
- [4] Bouwmeester, D., Pan, J.-W., Mattle, K., Eibl, M., Weinfurter, H., & Zeilinger, A. (1997, December 1). *Experimental quantum teleportation*. *Nature News*. Retrieved May 6, 2022, from <https://www.nature.com/articles/37539>
- [5] Briegel, H.-J., Dür, W., Cirac, J. I., & Zoller, P. (1998, December 28). *Quantum repeaters: The role*

- of imperfect local operations in quantum communication. *Physical Review Letters*. Retrieved May 6, 2022, from <https://doi.org/10.1103/physrevlett.81.5932>
- [6] Dong, S., Yu, Y., Zheng, S., Zhu, Q., Gai, L., Li, W., & Gu, Y. (2022, March 9). Practical underwater quantum key distribution based on Decoy-State BB84 protocol. *arXiv.org*. Retrieved April 27, 2022, from <https://arxiv.org/abs/2203.04598>
- [7] Gisin, N., Ribordy, G., Tittel, W., & Zbinden, H. (2002, March 8). *Quantum cryptography*. *Reviews of Modern Physics*. Retrieved April 27, 2022, from <https://journals.aps.org/rmp/abstract/10.1103/RevModPhys.74.145>
- [8] Gisin, N., & Thew, R. (n.d.). *Quantum Communication*. *Nature News*. Retrieved May 6, 2022, from <https://www.nature.com/articles/nphoton.2007.22>
- [9] Gupta, P. C. (2014). *Data Communications and Computer Networks*. PHI Learning.
- [10] Hufnagel, F., Sit, A., Bouchard, F., Zhang, Y., England, D., Heshami, K., Sussman, B. J., & Karimi, E. (2020, April 9). Underwater quantum communication over a 30-meter flume tank. *arXiv.org*. Retrieved May 6, 2022, from <https://arxiv.org/abs/2004.04821>
- [11] Ikuta, T., & Takesue, H. (2018, January 16). Four-dimensional entanglement distribution over 100 km. *Nature News*. Retrieved May 6, 2022, from <https://www.nature.com/articles/s41598-017-19078-z>
- [12] Jacobs, B. C., Pittman, T. B., & Franson, J. D. (2002, November 15). Quantum relays and noise suppression using linear optics. *Physical Review A*. Retrieved April 27, 2022, from <https://journals.aps.org/pra/abstract/10.1103/PhysRevA.66.052307>
- [13] Lükkenhaus, N., Calsamiglia, J., & Suominen, K.-A. (1999, May 1). Bell measurements for teleportation. *Physical Review A*. Retrieved April 27, 2022, from <https://journals.aps.org/pra/abstract/10.1103/PhysRevA.59.3295>
- [14] Liao, S.-K., Cai, W.-Q., Liu, W.-Y., Zhang, L., Li, Y., Ren, J.-G., Yin, J., Shen, Q., Cao, Y., Li, Z.-P., Li, F.-Z., Chen, X.-W., Sun, L.-H., Jia, J.-J., Wu, J.-C., Jiang, X.-J., Wang, J.-F., Huang, Y.-M., Wang, Q., ... Pan, J.-W. (2017, August 9). Satellite-to-ground quantum key distribution. *Nature News*. Retrieved May 6, 2022, from <https://www.nature.com/articles/nature23655>
- [15] Liu, C., Dutton, Z., Behroozi, C. H., & Hau, L. V. (n.d.). Observation of coherent optical information storage in an atomic medium using halted light pulses. *Nature News*. Retrieved May 6, 2022, from <https://www.nature.com/articles/35054017>
- [16] Lvovsky, A. I., Sanders, B. C., & Tittel, W. (n.d.). Optical quantum memory. *Nature News*. Retrieved May 6, 2022, from <https://www.nature.com/articles/nphoton.2009.231>
- [17] Ma, X., Qi, B., Zhao, Y., & Lo, H.-K. (2005, July 20). Practical decoy state for Quantum Key Distribution. *Physical Review A*. Retrieved April 27, 2022, from <https://journals.aps.org/pra/abstract/10.1103/PhysRevA.72.012326>
- [18] Neumann, S. P., Buchner, A., Bulla, L., Bohmann, M., & Ursin, R. (2022, March 23). Continuous entanglement distribution over a transnational 248 km fibre link. *arXiv.org*. Retrieved April 27, 2022, from <https://arxiv.org/abs/2203.12417>
- [19] Yoshizawa, A., Kaji, R., & Tsuchida, H. (2004, May 3). Gated-mode single-photon detection at 1550 nm by discharge pulse counting. *AIP Publishing*. Retrieved April 27, 2022, from <https://aip.scitation.org/doi/10.1063/1.1738176>
- [20] Zukowski, M., Zeilinger, A., Horne, M., & Ekert, A. (1993, December 1). "event-ready-detectors" Bell experiment via entanglement swapping. *Physical Review Letters*. Retrieved May 6, 2022, from <https://ora.ox.ac.uk/objects/uuid:c9eed79b-4854-4c00-a725-ae2ec2cf317d>